Environ Monit Assess (2013) 185:8239–8258
DOI 10.1007/s10661-013-3170-y

Heat wave hazard classification and risk assessment using artificial intelligence fuzzy logic

Iphigenia Keramitsoglou · Chris T. Kiranoudis · Bino Maiheu · Koen De Ridder · Ioannis A. Daglis · Paolo Manunta · Marc Paganini

Received: 30 April 2012 / Accepted: 25 March 2013 / Published online: 27 April 2013

Abstract The average summer temperatures as well as the frequency and intensity of hot days and heat waves are expected to increase due to climate change. Motivated by this consequence, we propose a methodology to evaluate the monthly heat wave hazard and risk and its spatial distribution within large cities. A simple urban climate model with assimilated satellite-derived land surface temperature images was used to generate a historic database of urban air temperature fields. Heat wave hazard was then estimated from the analysis of these hourly air temperatures distributed at a 1-km grid over Athens, Greece, by identifying the areas that are more likely to suffer higher temperatures in the case of a heat wave event. Innovation lies in the artificial intelligence fuzzy logic model that was used to classify the heat waves from mild to extreme by taking into consideration their duration, intensity and time of occurrence. The monthly hazard was subsequently estimated as the cumulative effect from the individual heat waves that occurred at each grid cell during a month. Finally, monthly heat wave risk maps were produced integrating geospatial information on the population vulnerability to heat waves calculated from socio-economic variables.

Keywords Heat wave · Fuzzy logic · Satellite images · Urban climate

I. Keramitsoglou (✉) · I. A. Daglis
Institute for Astronomy, Astrophysics, Space Applications and Remote Sensing, National Observatory of Athens, Metaxa & Vassileos Pavlou Str GR 152 36 Palea Penteli Athens, Greece
e-mail: ik@noa.gr

I. A. Daglis
e-mail: daglis@noa.gr

C. T. Kiranoudis
School of Chemical Engineering, National Technical University of Athens,
Zografou Campus GR 157 80 Athens Greece
e-mail: kyr@chemeng.ntua.gr

B. Maiheu · K. De Ridder
VITO Flemish Institute for Technological Research, Boeretang 200 B-2400 Mol Belgium

B. Maiheu
e-mail: bino.maiheu@vito.be

K. De Ridder
e-mail: koen.deridder@vito.be

P. Manunta
Planetek Italia S.r.l., via Massaua 12-70132 Bari Italy
e-mail: manunta@planetek.it

M. Paganini
European Space Agency, ESRIN,
Via Galileo Galilei, Casella Postale 64 I-00044 Frascati Italy
e-mail: Marc.Paganini@esa.int

Introduction

Heat waves are extended periods of extremely hot weather that have a major impact on human health, socio-economics and natural systems. According to the

European Environmental Agency in the decade between 1998 and 2009, heat waves were the most prominent hazard in Europe causing more than 70,000 excess deaths during the extreme summer of 2003 (EEA 2010). Extreme temperature events are normal features of inter-annual temperature variability, but their frequency and intensity have increased both in SW, Midwest and SE United States, in Western and Central Europe as well as in Mediterranean regions (EEA 2010; Meehl and Tibaldi 2004). Furthermore, the Intergovernmental Panel on Climate Change (IPCC 2007) projected impacts included a 'very likely' increase in frequency of heat extremes and heat waves in Europe (WMO 2011). North American 'cities that currently experience heat waves are expected to be further challenged by an increased number, intensity and duration of heat waves during the course of the century, with potential for adverse health impacts'. Increased attention has been drawn to natural hazards and the European Commission recently has published guidelines (EC 2010) for risk assessment and mapping for appropriate disaster management following a Council Conclusions call (Council of the European Union 2009).

The main purpose of these guidelines was to improve coherence and consistency among the risk assessments undertaken in the Member States at national level in the prevention, preparedness and planning stages and to make these risk assessments more comparable between Member States. Coherent methods for national risk assessments will support a common understanding in the EU of the risks faced by Member States and the European Union and will facilitate co-operation in efforts to prevent and mitigate shared risks, such as cross-border risks. The guidelines emphasise the need for national assessments to address the following subjects: (1) hazard analysis, including geographical, temporal and probability analysis and (2) vulnerability analysis taking into consideration population exposure as well as physical, economic, environmental and other social/political factors.

According to the World Meteorological Organization (WMO 2008), public health outcomes of hot weather and heat waves depend upon the level of exposure (frequency, severity and duration), the size of the exposed population and the population sensitivity. Heat waves and hot weather are potentially fatal and can aggravate existing health conditions. Health effects can appear in all age groups; however, some people are more at risk of heat-related illness and death than others. Variations in risk are related to individual conditions, the level of exposure to hot weather and heat waves and the ability to adapt to hot weather conditions.

Heat-related health impacts are largely preventable if populations, health and social care systems and public infrastructure are prepared (WMO 2008).This is plausible if past events are studied for which heat wave risk assessment and mapping are central components. Identifying the specific locations where certain population groups particularly vulnerable to heat stress live is beneficial for targeting public health interventions. The delineation of high risk zones is critical for the adaption of effective targeted measures in areas of public and private activity rather than in the whole city agglomeration. The evaluation of extreme events may support decision makers, stakeholders and interested parties to agree on the preventive measures to take and to prepare in ways to avoid the immediate heat wave consequences, most notably in citizens' health as well as energy demand in future events.

Therefore, in order to answer how severe a heat wave is, an expert will have to consider the intra-urban variability of the hazard, as well as the local socio-economic factors and their geographical variation. In that context, the present paper proposes a fuzzy logic methodology to assess heat wave hazard and the associated risk in the summer months. In this article we use the term 'hazard' to refer to the severity of a heat wave phenomenon and 'risk' to refer to the potential harm associated with the hazard. A fully automated system for the classification of heat waves that resembles the common perception of severity according to intensity, duration and time lag between events has been developed based on fuzzy logic. Additionally, the spatial distribution of socio-economic factors at census block scale is considered to estimate the associated risk. The methodology is applied to past events for the city of Athens, Greece, and considers the severity of the events at intra-urban scale.

The remainder of the paper is organised as follows: "Background" gives the necessary background with regard to heat waves and urban climate modeling, followed by a presentation of the case study area of Athens in "Athens Greater Area" and the datasets used for the development of the methodology in "Data". The methods employed for modeling the air temperature and building the fuzzy logic risk model are introduced in "Methods". Finally, the results of the application of the approach together with a sensitivity analysis are given in "Application" and the conclusions in "Conclusions".

Background

Heat waves

Morbidity and mortality increase during times of unusually high ambient air temperatures even in temperate climates (Armstrong et al. 2011). It is also widely found that the nature of the temperature–mortality relationship varies between places (e.g. Basu 2009; McMichael et al. 2008). Heat-related mortality is often underestimated and may only be indicated when heat waves occur, resulting in a signal detection bias. The studies to date are often limited by information from the death certificates. Other related information, such as income level, poverty, medicine use, time-activity patterns or air conditioning use, is not offered on the individual level, making it difficult to assess socioeconomic and health status of the casualties (Basu 2009).

Regarding spatial patterns, Henschel et al. (1969) and Schuman (1972) are among the first to investigate the spatial distribution of heat-related mortality rates. Recently, Johnson and Wilson (2009) commented that the spatial analysis of vulnerability to heat waves at intra-urban scale has been limited, with some exceptions including Harlan et al. (2006) and Smoyer (1998) that developed a multiple linear regression model using the Urban Heat Island (UHI) intensity and vulnerable population characteristics to predict heat-related mortality. Later Ruddell et al. (2010) illustrated that temperatures vary significantly within the same urban area, and that some residents are at significantly greater risk of exposure to threshold temperatures than others. They simulated a heat wave event of 4 days in Phoenix, AZ, using the WRF model (Shamrock et al. 2005) together with an urban surface energy balance model and showed marked contrasts in temperature across neighborhoods.

Urban agglomerations are especially vulnerable to heat waves in terms of increased mortality due to the so-called urban heat island effect (Dousset et al. 2011). Many factors contribute to this effect (Oke et al. 1991): Construction materials typically have a high heat storage capacity, causing prolonged heat release during night time; lack of evaporating surfaces yields a reduced latent heat flux and therefore an elevated sensible heat flux which causes an increased heating of the atmosphere; urban morphology plays a significant role as well, where the geometry of street canyons reduces the effective albedo of an urban surface as well as decreases the long wave radiation loss due to the screening of the skyline.

Heat wave hazard varies within a metropolitan area due to different topography, land cover/ land use, meteorological conditions (e.g. sea breeze) and the presence of UHI. On the other hand, population vulnerability to heat waves varies with age—with elderly people and infants being more vulnerable to high temperatures—and it is higher in urban areas due to higher population numbers and density (EEA 2010). On top of that, air pollution exacerbates the adverse health effect of higher temperatures, by stressing the respiratory and circulatory systems. It was recently shown (Dousset et al. 2011; Laaidi et al. 2011) using data from Paris 2003 that elderly people's mortality risk is significantly associated with exposure to the elevated minimum temperatures averaged over 2 weeks and averaged on the day of death and the six preceding days. Poverty and isolation are also influential factors. Housing characteristics (e.g. lack of thermal insulation) plays an important role as well. In addition to elevated mortality, serious illnesses, such as heat stroke, heat exhaustion, cardiovascular, and respiratory problems, rise during the warmest spells of the year (Semenza et al. 1999). Deaths and illnesses from air pollutants and infectious diseases also increase during extremely hot weather (Easterling et al. 2000; Patz et al. 2005).

Urban climate models

Typical modeling exercises employ regional climate models coupled to an urbanised surface module to account for the presence of cities. Several models exist to compute the surface heat fluxes (De Ridder and Schayes 1997; Grimmond and Oke 2002; Masson 2000; Kusaka et al. 2001; Ca et al. 2002; Martilli et al. 2002; Dupont and Mestayer 2006; De Ridder 2006). Nevertheless, such fully coupled modeling approaches tend to be computationally prohibitive to generate the required urban air temperature fields at the spatial resolution of ~1 km during the course of multiple summer seasons. As an alternative, studies on urban climate may employ statistical techniques typically involving methods like regression analysis or kriging in which satellite-derived land surface temperature (LST) retrievals are used as in situ estimations of the urban temperature fields (Gallo and Owen 1999; Jarvis and Stuart 2001a, b; Choi et al. 2003). In this

paper, we propose the modeling approach developed by VITO, the Flemish Institute for Technological Research in Belgium (Maiheu et al. 2010; Manunta et al. 2010a; Keramitsoglou et al. 2012) which is based on a simple urban climate model constrained by satellite LST retrievals via data assimilation and embedded in the coarse resolution European Centre for Medium-Range Weather Forecasts (ECMWF) Interim reanalysis data (ERA-Interim, see "Ancillary data").

Athens Greater Area

Athens is the capital and largest city of Greece. According to the recent census paper of Eurostat (http://epp.eurostat.ec.europa.eu/), the Athens Larger Urban Zone (LUZ) is the eighth most populated LUZ in the European Union with a population of about 4,000,000. Athens is characterised by a warm thermo-Mediterranean climate with mild and relatively wet winters and warm dry summers. The average air temperature of the warmest month (July) is 28 °C. The City of Athens is the central municipality with a population density of 20,467 people/km^2. Athens is a coastal city at the south-easternmost edge of the Greek mainland (Fig. 1) which sprawls across a central basin bound by Mount Egaleo to the west, Mount Parnitha in the north, Mount Penteli in the northeast, Mount Hymettus in the east and the Saronic Gulf in the southwest. The basin is bisected by a series of small hills. These specific topographic characteristics make Athens an example of a coastal city located in very complex terrain.

Analysis of 9 years of MODIS acquisitions (Keramitsoglou et al. 2011) revealed three areas that consistently appeared warmer than the city centre in the daytime images. These areas are Megara, Elefsina-Aspropyrgos and Mesogeia which were mainly covered by sparse low vegetation and bare soil (negative heat island). On the other hand, the city centre of Athens was characterised by a strong surface Urban Heat Island phenomenon of 5.7 °C in average, which was observed later in the day and mostly at night-time spatially coinciding with the dense urban fabric.

With air temperatures often rising above 37 °C in Athens, heat waves are not seldom episodes. A major heat wave in Athens in 1987 was associated with more than 2,000 deaths (Katsouyanni et al. 1988). The combination of large-scale subsidence and horizontal movement of air masses from southern parts is the typical cause of the heat wave phenomenon over Greece (Theoharatos et al. 2010).

During the last 10 days of June and July 2007, Athens experienced two extreme heat events. Those heat waves became front page news in all Greek newspapers, and the Public Authorities took preventive measures. The National Health's Operational Centre (NHOC) declared a state of national alert from June 22 to June 28 and from July 23 to 27 (Theoharatos et al. 2010). During the first 2 weeks of June 2007, daily maximum air temperature in Athens varied within its normal values (from June to August daily maximum temperature at Athens is 31.6 °C, with reference to 1961–1990 period; Founda and Giannakopoulos 2009; Theoharatos et al. 2010) and started to rise gradually above normal during the third week, when the area was affected by the first and most severe heat wave of the summer from 24 to 28 June 2009 (Founda and Giannakopoulos 2009) reaching air temperatures as high as 46 °C. Two night-time MODIS LST images depicting the LST distribution before and during the event using the same color scale are indicative of the severity of the June heat wave (Fig. 2a and b). Due to high temperatures coupled with strong winds, several fires raged across central and southern Greece, and Athens was covered in a cloud of thick black smoke as a large fire on Mount Parnitha caused significant parts of the National Park to be destroyed. The fire is identifiable on the LST image of 28 June, north of the centre of Athens (Fig. 2c).

Data

Thermal infrared satellite data

An important ingredient for the heat wave risk assessment and mapping is the availability of hourly and spatially explicit urban air temperature data. The availability of dense measurement networks would be indispensable to capture the spatial distribution of temperature and humidity in urban environments. However, the existing urban meteorological networks only cover limited areas—often away from the city centres—and are therefore not adequate to capture the spatial variability of the temperature within a complex urban environment. Satellite sensors of ~1 km spatial resolution can provide a few images of LST per day

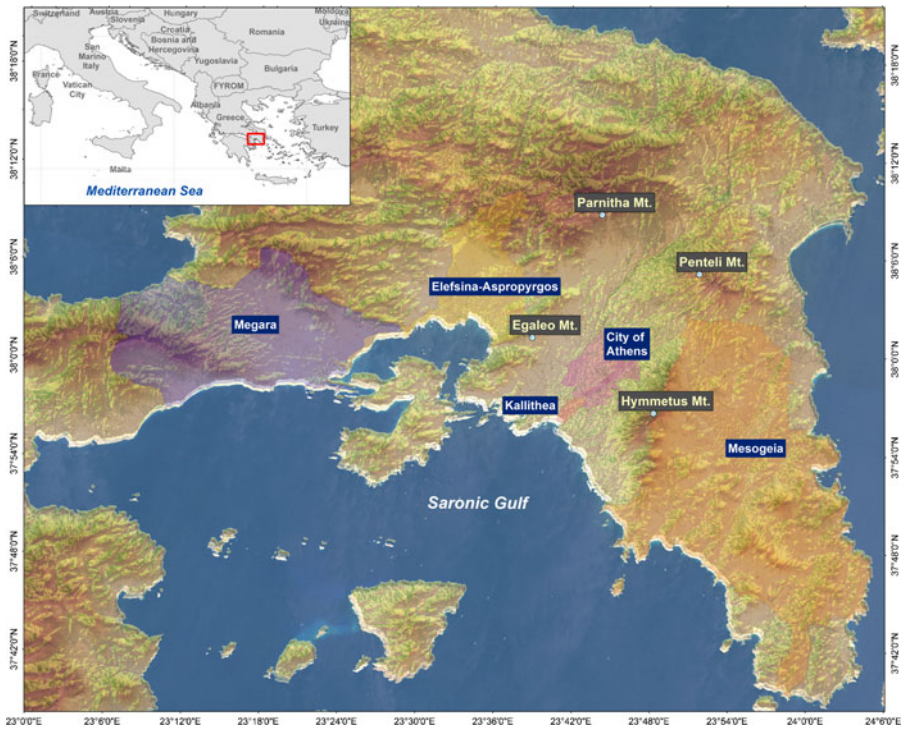

Fig. 1 Athens, Greece, with areas of interest on the map. The *red mark* denotes the location of the National Observatory of Athens in Thission

both during day- and night-time. The most commonly used instruments with thermal infrared bands at this resolution include NOAA/AVHRR (National Oceanic and Atmospheric Administration/Advanced Very High Resolution Radiometer) and Terra, Aqua/MODIS (MODerate-Resolution Imaging Spectroradiometer). Envisat/(A)ATSR (Advanced Along-Track Scanning Radiometer) data are available until 8 April 2012 when communication with Envisat satellite was lost. Although rich in spatial detail for the scale under consideration here, the limited revisit time of these sensors is still not sufficient for monitoring the diurnal variation at any given area. One therefore has to rely on modeling approaches.

In the present study, we analysed a 3-year time series of MODIS summer images (from May to October 2007–2009) acquired over Athens. Specifically, 415 daytime MODIS-Terra LST maps and 319 MODIS-Terra and Aqua LST maps were produced and archived as part of the requirements of Urban Heat Islands and Urban Thermography project (21913/08/I-LG) funded by the European Space

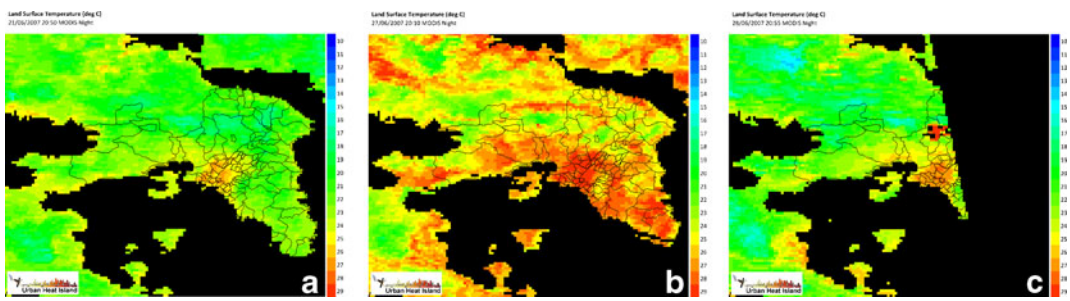

Fig. 2 Sequence of satellite-derived LST maps from MODIS 1 km spatial resolution images around midnight local time depicting one of the most intensive heat wave events of the recent history: **a** typical LST image of Athens acquired 1 day before the event started (21 June 2007); **b** the night with highest temperatures at the peak of the event (27 June 2007); and **c** Parnitha National Park of Greece destructive wildfire due to high temperatures and strong winds (28 June 2007) [Data Source: ESA UHI Project Grant No. 21913/08/I-LG]

Agency ('the UHI project' hereafter; Manunta et al. 2010b; http://www.urbanheatisland.info). The original MODIS data used in the present study were procured at no charge from the Warehouse Inventory Search Tool (WIST web site) repository. MODIS is a key instrument on board the Terra (EOS AM) and Aqua (EOS PM) satellites. Terra's orbit around the Earth is timed so that it passes from north to south across the equator in the morning, while Aqua passes south to north over the equator in the afternoon. MODIS has 20 infrared bands; however, two of them are suitable for LST retrievals, namely, bands 31 and 32 at 11.0 and 12.0 μm, respectively. The spatial resolution of TIR bands is approximately 1 km at nadir. The production of LST images is described in Keramitsoglou et al. (2011). These LST images were subsequently assimilated into the Urban Climate Model (Urban Climate Model).

Ancillary data

The lateral boundary conditions for the urban climate model are given by the ECMWF ERA-Interim dataset (Dee et al. 2011), thereby accounting for the large scale temperature and wind field variations. Down-welling long- and shortwave surface radiation fluxes needed for the urban energy budget are interpolated from the corresponding Land Surface Analysis Satellite Applications Facility datasets (LSA SAF 2010; 2011). These data are given at the spatial resolution of the Meteosat Second Generation Spinning Enhanced Visible and Infrared Imager (SEVIRI) instrument, typically 4–5 km resolution at the latitude considered. Land cover information was derived from the CORINE land cover dataset by the European Environmental Agency (EEA; www.eea.europa.eu). More specifically, we derived the fraction of sealed (urban) surface and the fraction of water content in each model grid cell from this dataset. The vegetation fraction was derived from the 10-day syntheses SPOT-VEGETATION Normalized Difference Vegetation Index data made available through the VITO VEGETATION archive (http://free.vgt.vito.be). The model thereby accounts for the change in vegetation cover during the course of a summer period. Terrain elevation data at 1 km resolution were derived from the US Geological Survey (USGS) GTOPO 30 dataset, available from the USGS Earth Resources Observation and Science Center. Note that all ancillary data needed in the urban climate modeling approach are freely obtainable.

Census data

Vulnerability of population was estimated at the finest available level using census block datasets from the general population census of 2001. This was the most recent one at the time of methodology development. In particular, population density and percentage of non-proper dwellings were the two variables from the census. A vector file containing the geographic boundaries of the census blocks of the study area was employed to illustrate the data (Fig. 3). The vector dataset were joined with the population living in the blocks and the number of non-proper dwellings. These include sub-standard dwellings made of inexpensive construction materials without a predetermined design plan. This information was provided by the Hellenic Statistical Authority (www.statistics.gr).

In situ data

A ~20-year time-series of air and dew point temperatures was collected from the Meteorological & Actinometric Station of the National Observatory of Athens (NOA), located on the Hill of Nymphs at Thission area in the centre of Athens (Fig. 1; position, 38° 0.00′ N, 23° 43.48′ E, height above sea level 110 m; operated by the Institute of Environmental Research and Sustainable Development). A long time series is necessary to calculate meaningful statistics for the city under consideration and establish dynamic thresholds that characterise that particular city (see Identification and extraction of Hot Days; Table 1).

Methods

Concept

According to the International Organization for Standardization (ISO 31010), indices can be used for classifying different risks associated with an activity if the system is well understood. They permit the integration of a range of factors which have an impact on the level of risk into a single numerical score for level of risk. The inputs are derived from analysis of the system, or a broad description of the context. This

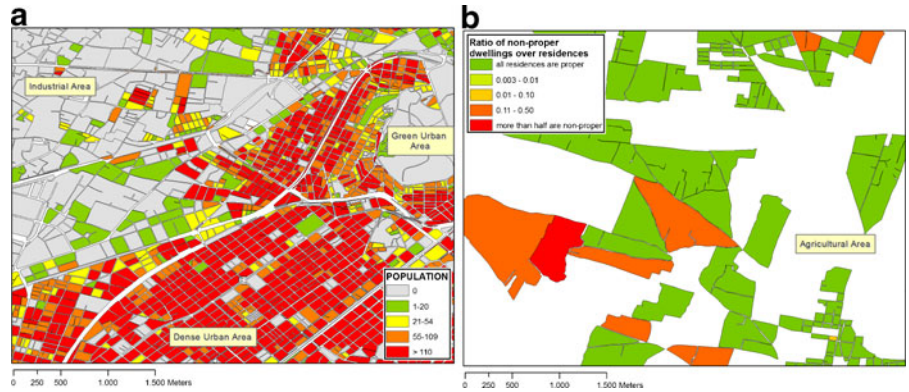

Fig. 3 Indicative subsets of census data showing the population near Athens centre (on the *left*) and the ratio of non-proper dwellings over all residences per census block in an agricultural area (on the *right*) [Source: Hellenic Statistical Authority]

requires an adequate understanding of all the sources of risk, the possible pathways and what might be affected. Tools such as fault tree analysis, event tree analysis and general decision analysis can be used to support the development of risk indices. Once the system has been defined, scores are developed for each component in such a way that they can be combined to provide a composite index. Cumulative effects can be taken into account by adding scores. Uncertainty can be addressed by sensitivity analysis and varying scores to find out which parameters are the most sensitive.

Based on the above understanding, the methodology adopted here is illustrated in Fig. 4. MODIS acquisitions in the infrared electromagnetic spectrum ("Thermal Infrared satellite data") were processed so as to derive LST images. These LST instances (two to three per day) were then assimilated into an urban climate model ("Urban climate model"), which also took into account other ancillary data ("Ancillary data"), to reconstruct the air temperature 3D field for three summers (2007–2009). The two-dimensional spatial grid (latitude–longitude) was 1 km, whilst the temporal step represented hourly intervals. In situ data ("In situ data") from a long ground station record (~20 years) was used to dynamically define relevant statistical thresholds, which were then used to extract the hot days from the 3D air temperature grid ("Identification and extraction of hot days). Subsequently, heat wave events were identified, and relevant parameters were calculated, including their intensity, duration and time lag between two consecutive events. Artificial intelligence fuzzy logic was then used to characterise each heat wave event from mild to extreme (Classification of heat wave events). The accumulated monthly result was the monthly spatial distribution of heat wave hazard ("Monthly heat wave risk"). This information was then convoluted with the spatial distribution of population vulnerability to heat waves ("Population vulnerability to heat waves" using census data presented in "Census data") to provide the final product, namely the monthly spatial distribution of heat risk.

Urban climate model

The air temperatures used for the heat wave risk model were generated by an urban climate model developed at VITO (Maiheu et al. 2010). The main criteria for model selection were: (1) speed, as the model had to produce long historic time series of urban air temperatures for ten European cities and (2) usage of freely available ancillary data.

The model consisted of two separate components, namely a surface module that computes spatially

Table 1 1991–2009 Air temperature statistics using ground measurements in the centre of Athens, where T_{appmax}: the maximum apparent temperature, T_{min}: minimum air temperature, p90: 90th percentile, p95: 95th percentile

Month	T_{appmax}.p90	T_{appmax}.p95	T_{appmax}.median	T_{min}.p90	T_{min}.p95
May	30.4	32.0	25.4	20.4	21.2
June	36.6	37.9	31.6	25.2	26.2
July	39.9	41.9	34.9	26.8	27.4
August	39.4	40.7	34.7	26.7	27.7
September	34.1	35.5	29.6	23.2	24.0

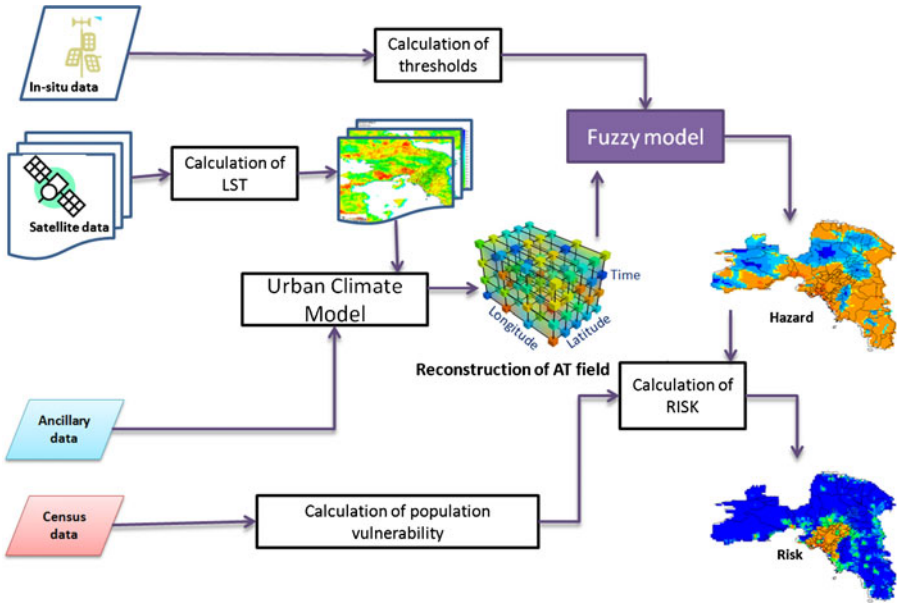

Fig. 4 Conceptual flowchart of the methodology proposed for the calculation of heat wave risk

explicit sensible heat fluxes and a second, atmospheric component which ingests these fluxes as a lower boundary condition and computes the vertical diffusion and horizontal advection of the air temperature. The surface model consisted of a two-layer prognostic force-restore soil temperature model (Garratt 19922). Here, the soil heat flux was replaced in the urban environment by the storage heat flux computed by the objective hysteresis model (OHM; Grimmond and Oke 2002), taking into account the net radiation balance at the surface using downwelling radiation fluxes provided by LandSAF. The relationships given by Grimmond and Oke (2002) which were based on the parameterisations by de Bruin and Holtslag (1982) were used to compute the turbulent sensible and latent heat fluxes. The surface module uses CORINE land cover to derive sealed surface fraction and water content in every grid cell; vegetation fraction is derived from 10-day SPOT-VEGETATION composites in order to allow for seasonal effects in NDVI.

OHM coefficients were derived based on Grimmond and Oke (2002), Rigo and Parlow (2007) and Roberts et al. (2006); however, as they are typically expressed for material types, it proved rather difficult to specify appropriate values for generic urban environments due to the large variation of the coefficients in literature. Therefore, an additional constraint was built into the model via ensemble data assimilation. In a sequential Monte Carlo (Doucet et al. 2001) method, the MODIS LST observations were compared with the model's surface temperature fields. The model fields were subsequently adjusted via importance sampling to better match with the observed LST retrievals. In this technique, an ensemble of model states was generated and propagated in time using the model's dynamic equations.

At times when MODIS LST retrievals were available, weights were assigned to each of the model states, reflecting the conditional likelihood for that particular model state given the observation. During the assimilation or analysis step in the procedure, model states were drawn from the ensemble available at that time, taking into account the relative likelihoods. A new ensemble of model states which better reflected the satellite-retrieved LST patterns was thereby constructed.

The atmospheric module used wind speed and direction as well as air temperature derived from ECMWF ERA Interim reanalysis as lateral boundary conditions. A single wind vector and temperature value was applied to the whole domain on an hourly basis in order to calculate horizontal advection and vertical diffusion of the air temperature. The sensible heat fluxes from the surface module described above were used as lower boundary conditions. The model was able to run relatively fast but did not allow local circulations such as an urban-breeze to develop. It is important to mention that the air temperature model does not take into account microscale effects and can

therefore be thought to be representative for the inertial sublayer above a certain blending height in which the effects of individual roughness elements and street canyons are aggregated (Oke 2006). A more detailed description of the air temperature modeling approach can be found in Maiheu et al. (2010), Manunta et al. (2010a) and Keramitsoglou et al. (2012).

As the model generated long historic time-series of urban air temperatures, statistical analyses became possible. An example of the 90th percentile for the UHI effect in Athens during June 2007 is shown in Fig. 5. The map represents for that particular month the local temperature increment of the urban area compared with the rural background temperature at 20:00 UTC, roughly corresponding to the time of the day when the UHI effect is most pronounced. The UHI intensity was then defined as the air temperature offset in each pixel with reference to the median of the air temperature in the rural pixels. Note that both temperatures were corrected for altitude using the standard lapse rate of −6.5 K/km. We clearly see the most extreme urban temperature increments, up to 6 °C (90th percentile), over the denser urban fabric.

Heat wave hazard and risk

Identification and extraction of hot days

Due to the fact that heat waves are defined relatively to the usual weather conditions in a given area, there is no universal definition of a heat wave (EEA 2010), e.g. in terms of a fixed temperature threshold that has to be reached for a number of consecutive days. Nevertheless, suggestions for a generic definition do exist. In the present work, such a universal definition was adopted as proposed by the EuroHEAT project (Improving Public Health Responses to extreme weather/heat-waves). According to it, a day is characterised as a 'hot day' based on values of maximum apparent temperature (T_{app}) and high night-time temperatures through minimum temperature (T_{min}). T_{app} is a discomfort index based on air (AT) and dew

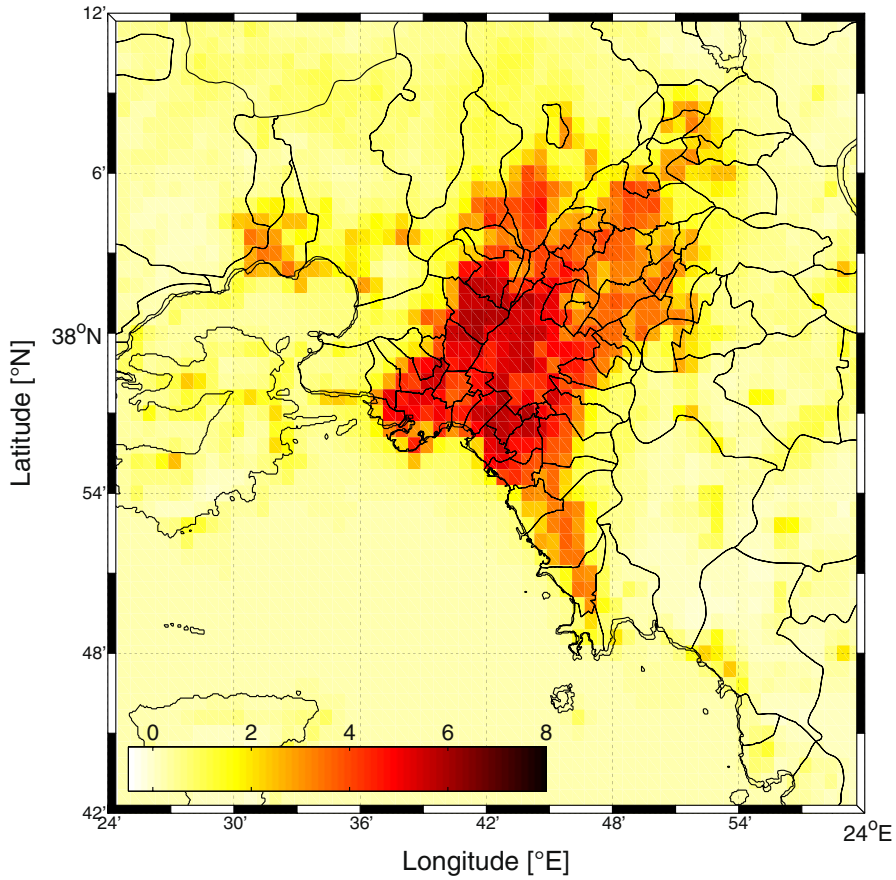

Fig. 5 Urban climate modeling result for Athens UHI effect during June 2007 based on the 90th percentile. The colours represent the UHI intensity in degrees Centigrade with reference to the median temperature over all rural pixels for that particular month

point (T_{dew}) temperatures, thus accounting for the physiological impact of heat on health. It is calculated using the following formula:

$$T_{app} = -2.653 + 0.994AT + 0.0153{T_{dew}}^2 \quad (1)$$

Hot days were then defined (D'Ippoliti et al. 2010) as days with either (1) T_{appmax} exceeding the 90th percentile of the monthly distribution or (2) days in which T_{min} exceeds the 90th percentile and T_{appmax} exceeds the median monthly value. In addition, we further adopted empirical rules for Athens, where a hot day is defined as a day during which the air temperature exceeded 37 °C for more than 3 h (Hellenic National Meteorological Service, HNMS, personal communication; Founda and Giannakopoulos 2009; Metaxas and Kallos 1980).

In order to calculate the above-mentioned dynamic thresholds necessary for the identification of hot days, a 20-year time series from NOA station at Thission was used. The climatological values that were used for the extraction of hot days and the estimation of heat wave intensity (see next in Classification of heat wave events) are shown in Table 1.

Following the extraction of hot days, the identification of heat waves was straightforward, as a sequence of two or more hot days. In the case that a series of hot days was interrupted by one non-hot day, then this was treated as one heat wave event.

Classification of heat wave events

One of the innovations of this analysis is the classification of the severity of the heat wave event resembling common perception based on several characteristics of the event using artificial intelligence fuzzy logic. Fuzzy logic theory has emerged over the last years as a useful tool for modeling processes which are too complex for conventional quantitative computing techniques to solve or when the available information from the process is qualitative, inexact or uncertain. Zadeh (1965) introduced the fuzzy logic theory, which only recently became a popular technique for developing sophisticated models and systems with numerous applications. The reason for this rapid development of fuzzy systems stems from some unique and powerful characteristics of fuzzy logic. It addresses qualitative information perfectly as it resembles the way humans make inferences and take decisions in a 'natural' way; 'natural' generally means in the language of the expert or the user. It fills an important gap in system design methods, which is between purely mathematical approaches (e.g. system design) and purely logic-based approaches (e.g. expert systems). While other approaches require accurate equations to model real-world behaviors, fuzzy design attempts to accommodate the ambiguities of real-world human language and logic. It provides an intuitive method for describing systems in human terms and automates the conversion of those system specifications into effective models. The fuzzy logic was used in this study to build a model for the classification of a heat wave event from mild to extreme based on important influencing factors. The Mamdani model was selected (Mamdani 1974), which describes process states by means of linguistic variables and uses these variables as inputs to control rules. The development of the system was completed in three steps:

The first step was the selection of input parameters to be included in the knowledge base of the expert system, a repository of human knowledge drawn from experience, published work or communication with experts. This was made so that all the important influencing factors were considered, while maintaining the system at a reasonable size. The parameters considered are presented below and were based on D'Ippoliti et al. (2010).

- Intensity: Heat wave intensity can be estimated in different ways, one approach being to consider the maximum air temperature, as a straightforward attribute routinely measured in every city and directly appreciated by non-experts. For Athens, we selected the 'psychological' air temperature threshold of 40 °C, above which almost all activities paralyse (Founda and Giannakopoulos 2009; HNMS personal communication). However, air temperature is clearly city-specific, therefore a more general statistical threshold was used as well, namely the deviation of T_{appmax} from the monthly T_{appmax}.p95 calculated using the 20-year station data (see Table 1). This attribute is of course more complicated to calculate, needs a long past record, but it is independent of the city. These two intensity attributes refer to the maximum daytime air temperature. It is noted that this threshold differs from the Hot Day definition one of T_{appmax}.p90, as it addresses 'how hot is a hot day'. Additionally, recent publications provided evidence that it is

actually unusually high night temperatures that have the most significant health impact (Dousset et al. 2011); therefore, we also considered the deviation of the T_{min} from the T_{min}.p95 as a measure of the heat wave intensity (see Table 1).

- Duration: Heat wave duration is the number of consecutive hot days. D'Ippoliti et al. (2010) showed results that give evidence for duration to play a more important role than intensity. Heat waves of long duration had the greatest impact on mortality and resulted in 1.5 to 3 times higher daily mortality than for other heat waves.
- Timing: It refers to the time lag since the previous event. The first heat wave of the season (starting on May 1st) is considered separately. Following that, any event occurring 3 days or less after a previous heat wave is considered to have an accumulative effect on the population.

The second step was the development of the database, where fuzzy sets were defined for all input parameters, as well as for the only output variable, namely, the severity of the heat wave event. The fuzzy sets appointed to each input or output variable are as follows:

- Input:
  - Intensity: Three triangular fuzzy sets, namely 'Low', 'Medium' and 'High' were defined on the input space which measured the maximum air temperature and compared it with the 'psychological' threshold of 40 °C to characterise the intensity. The example shown in Fig. 6a illustrates that using fuzzy sets seems more appropriate than the use of crisp thresholds. The linguistic variable 'Intensity' consisted of the terms 'Low', 'Medium' and 'High'. Other parameters (e.g. T_{appmax}, T_{min}) were also considered using the same concept.
  - Duration: The variable 'Duration' was described by three terms, namely 'Short', 'Long' and 'Extra Long' depicted by two triangular and one trapezoidal function, as presented in Fig. 6b.
  - Timing: In this case, two fuzzy sets (terms) were defined on the input space. One triangular named 'High effect' and one trapezoidal named 'No effect'.
- Output: heat wave hazard: The only output variable was the characterisation (classification) of the severity of the heat wave event, and it was measured from 0 to 5. The higher the number, the more extreme the event. Simple 5- or 6-integer category classifications exist for a number of hazards. These classifications can help the general public to understand the magnitude of the event. Five triangular fuzzy sets were defined on the above-mentioned output space, namely 'Mild', 'Mild to

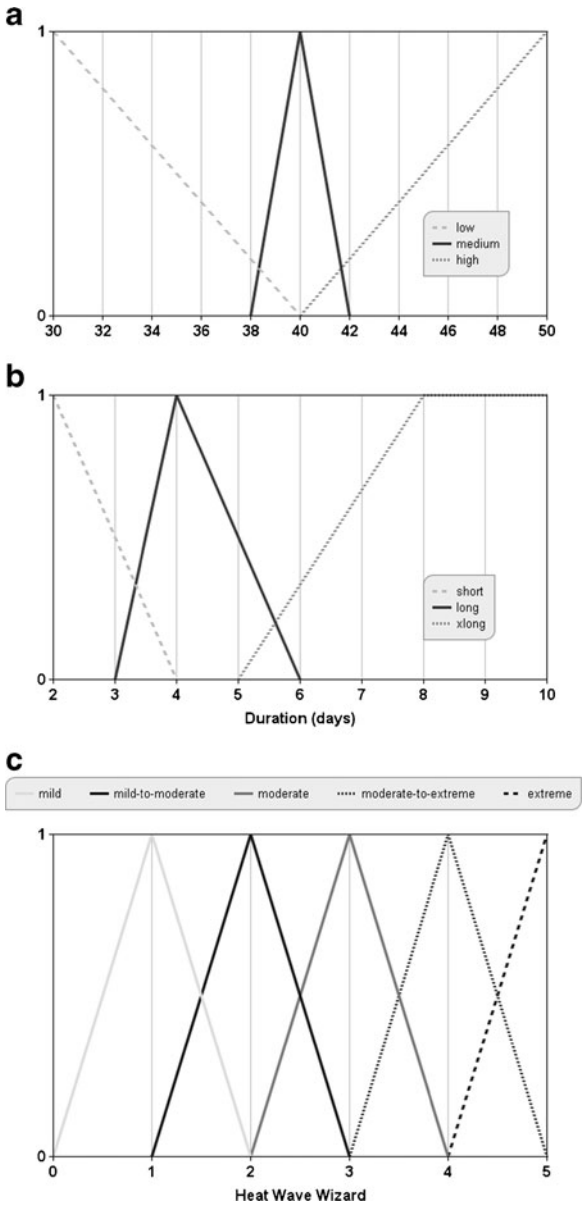

Fig. 6 Fuzzy sets defined for **a** input value "Intensity based on the psychological threshold of 40 °C", **b** "Duration", **c** output value heat wave hazard (severity)

moderate', 'Moderate', 'Moderate to extreme' and 'Extreme'. This is appropriately depicted in Fig. 6c.

The third step consisted of the development of the rule base. During this step, the experts developed a number of fuzzy rules, based on their intuition and experience. The rules connected the input variables with the output variable (heat wave hazard) and were based on the fuzzy state description that was obtained by the definition of the linguistic variables. The number of linguistic variables and the number of terms of each variable determined the number of rules. They were constructed in simple language terms and can be understood at a common sense level. At the same time, these rules yield specific and repeatable (same inputs gives same output) results. An example is given below:

> If a heat wave event is very long and the intensity is high and it happened soon after another heat wave, then the event is characterised as EXTREME.

The above three-step procedure defined the knowledge base of the fuzzy system. When the fuzzy model was to be applied to the set of input parameter values (crisp input values, e.g. AT_{max} is 43 °C, duration is 5 days and the events starts 2 days after the previous heat wave), the information flowed through the fuzzification–inference–defuzzification processes in order to classify the heat wave hazard. First, the fuzzification process transformed the crisp values into grades of membership for the participating fuzzy sets. Subsequently, fuzzy inference process combined the facts obtained from the fuzzification with the rule base and conducted the fuzzy reasoning process. Finally, defuzzification computed the final heat wave classification. The centroid defuzzification method (Driankov et al. 1993) was used, where the crisp value of the output variable was computed by finding the centre of area below the combined membership function.

Population vulnerability to heat waves

Age has been found (Basu 2009) to modify the association between ambient temperature and mortality. The elderly and children have been reported to be at greater risk from mortality following heat waves, as well as ambient temperature. Nevertheless, different studies have given the age thresholds of 75 years, or 65 years of age, children under 15 years, 5 years and younger, and infants 1 year of age and under to be at increased risk for mortality from high ambient temperature (see review in Basu 2009). As the number of infants, young children and the elderly is highly correlated with population density, a variable routinely provided from census data in cities, we took into consideration the latter to estimate population vulnerability. Another independent variable is the percentage of non-proper dwellings made of inexpensive materials without heat insulation.

The census datasets corresponding to population and housing were firstly joined with the vector census blocks dataset. Subsequently, they were mapped appropriately to the same 1-km grid as the hazard output. A fuzzy model was then developed for mapping the population vulnerability to heat waves taking into consideration two independent variables: (1) population density and (2) non-proper houses. The fuzzy sets appointed to each input or output variable are as follows:

- Input:
  - Population density: Three triangular fuzzy sets, namely 'Sparse', 'Medium' and 'Dense' were defined on the input space which measures the population density depicted by two triangular and one trapezoidal function. 'Sparse' is a grid point corresponding to population density less than 150 inhabitants per km^2, 'Medium' from 100–1,500 inhabitants/km^2 and 'Dense' above 1,000 inhabitants /km^2.
  - Ratio of non-proper dwellings over total number of residences: Essentially, this characterises the grid point as 'proper' if the ratio is below 0.5, i.e. more than half of the residences are proper.
- Output: heat wave population vulnerability: The only output variable was the characterisation of the population vulnerability to heat wave events, and it was measured from 0 to 20. The higher the number, the more vulnerable population is. Four triangular fuzzy sets were defined, namely 'Negligible', 'Low', 'Medium' and 'High'.

The resultant 1-km resolution vulnerability map for the case study area is presented in Fig. 7. Apart from the evident densely built-up centre, the other settlements around Athens as well as the coastal settlements are shown.

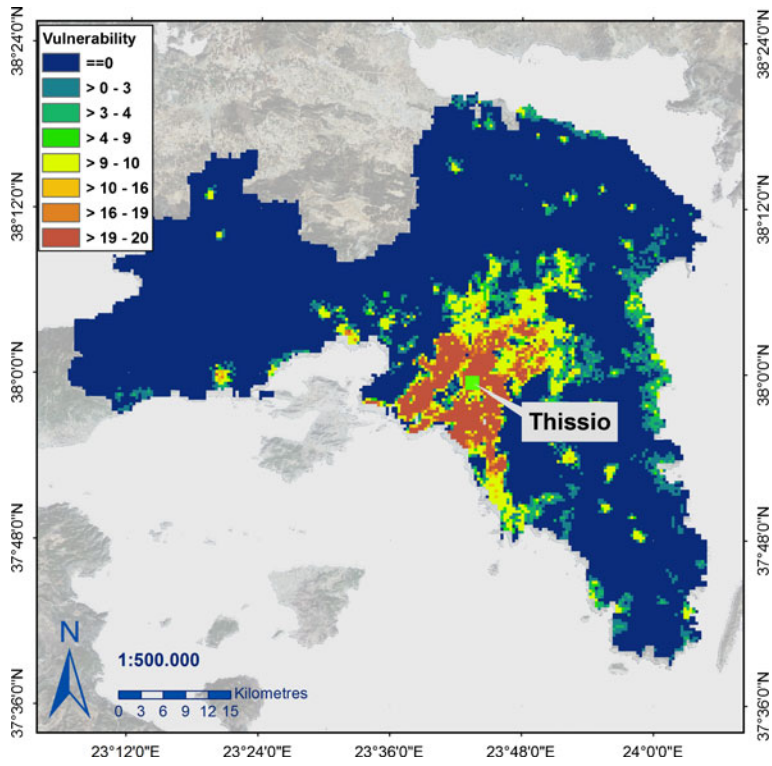

Fig. 7 Population vulnerability to heat waves at 1 km spatial resolution. The National Observatory of Athens station at Thissio from where we used the 20-year time series of meteorological data (In situ data) is marked on the map

Monthly heat wave risk

In order to calculate the heat wave hazard of a particular month, the event scores (see "Classification of heat wave events") for that month were added, yielding the monthly spatial distribution of heat wave hazard. This information was then multiplied by the spatial distribution of population vulnerability to heat waves to provide the final product, namely the monthly spatial distribution of heat risk.

Application

Results

The methodology presented in "Methods" was applied to three summers (2007–2009). The methodology and heat wave event classification was then applied to every grid point of the 3D air temperature field 'latitude–longitude-time' (grid step of '1 × 1 km × 1 h'). The monthly hazard and risk maps of the summer months (June, July, August) from 2007–2009 are shown in Fig. 8.

Figure 8 shows the distribution of the heat wave hazard within the study area exhibiting remarkable differences spatially mostly evident in the hot summer months of 2007. In the June 2007 map, the area of higher severity is more extended. The July 2007 map shows overall lower severity values than June. Recent investigation in the cause of the two exceptional events of June and July 2007 (Theoharatos et al. 2010) has provided evidence that the two heat waves had distinctly different thermo-hygrometric characteristics at the surface level, the event of June being hot and damp whilst the event of July hot and dry. Evidently, the hot and wet characteristics of the June event led to higher values of T_{app} (see Eq. 1). The pattern of hazard shows higher values in the central low-altitude municipalities in the Attica basin. The mountains surrounding the basin are shown as expected as low-hazard areas, due to the lower air temperatures.

Figure 9 shows the corresponding risk maps for the same months. A very interesting result is that the somehow familiar pattern of temperature (see also Fig. 2) is altered once the population vulnerability is convoluted to the hazard maps. The resulting risk maps show that the City of Athens and the areas around the centre with high population density are exposed to much higher risk than the adjacent

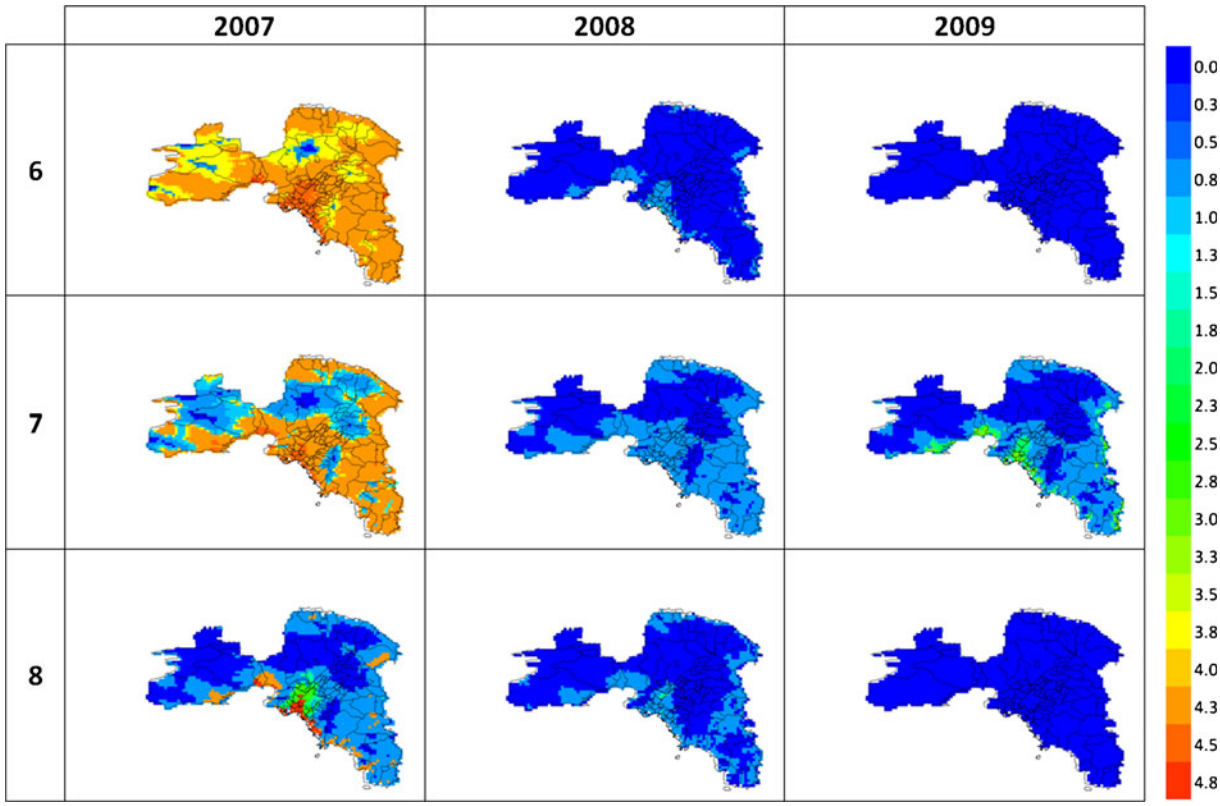

Fig. 8 Overview of heat wave hazard maps for Athens Greater Area for the summer months of 2007–2009 (*6*: June, *7*: July, *8*: August)

municipalities due to their high population vulnerability. The settlements around Athens are identifiable in the warmest months of June and July 2007 as areas of slightly increased risk. This pattern is evident due to the corresponding population. Another interesting feature at this scale is the relatively high values of risk at Elefsina-Aspropyrgos due to increased number of non-proper houses (Roma dwellings). The risk values are higher in June than in July.

At this stage, it is interesting to cite the health effects reported for the same period (published in Theoharatos et al. 2010). During the June event, NHOC reported 146 emergency department visits for heat exhaustion and heat stroke in Attica region and six deaths from excessive heat exposure. In July, there were a limited number of patients affected by the heat wave (46 patients and 1 death). The health data are not location-specific and therefore cannot be used for quantitative validation of our approach; nevertheless, they provide evidence that our overall result about the risk in June being higher than that of July is correct.

Validity of model's individual components

The accuracy of the heat wave risk and hazard maps in terms of spatial distribution can only be judged by taking into account the validity of the individual components used for the model and also by testing the fuzzy model itself in a number of ways. As far as the input components are concerned, the output of the urban climate model has been extensively validated within the framework of UHI project. The results for Athens using 15 months of hourly data from ten meteorological stations show that the model overestimated ground-based temperatures by an average of 1 °C (standard deviation 2 °C), whilst the mean temporal correlation coefficient for the entire validation dataset was equal to 0.911 (Manunta et al. 2011). In Keramitsoglou et al. (2012), results are presented of a validation using data from the THERMOPOLIS campaign (July 17, 2009–August 2, 2009; Daglis et al. 2010) using 26 monitoring sites spread out over the city. It was shown than the model was able to explain 85 % of the spatial variance

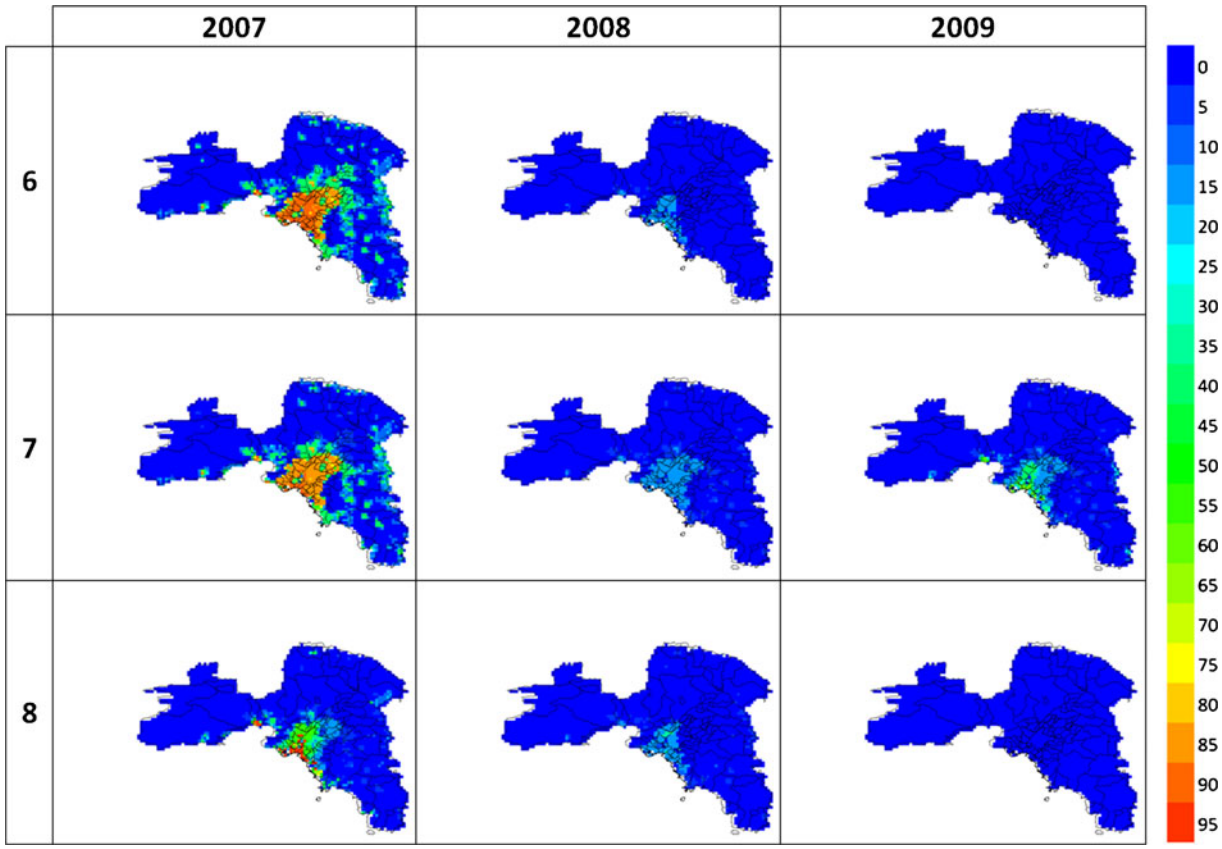

Fig. 9 Overview of heat wave risk maps for Athens Greater Area for the summer months of 2007–2009 (*6*: June, *7*: July, *8*: August)

of the average air temperatures measured during the campaign. During this period, the RMS difference between the average modeled and observed air temperature was 0.55 °C.

Socio-economic census data are considered accurate; however, since they are updated every decade, they are potentially up to 9 years out-of-date. For a growing city, this is an important factor of underestimating the population vulnerability. In addition, the fuzzy model has been extensively checked and fine-tuned using a long record of NOA station data. The model scored 100 % in detecting hot days and heat waves. The ultimate validation exercise is to compare the output hazard and risk maps against spatially distributed morbidity and mortality data; at the stage of publication and to the knowledge of the authors, such dataset is not available for Athens.

The system response was exhaustively tested regarding its ability to identify heat wave events and calculate correctly its attributes (duration, intensity, starting day, time lag between events) on the 20-year series from NOA station. The two heat waves of June and July 2007 were appropriately identified and classified as ‘extreme’ (hazard score: 4.7/5.0). A subset of the results is presented in Table 2.

Sensitivity analysis

There are often considerable uncertainties associated with the analysis of risk (ISO 31010). An understanding of uncertainties is necessary to interpret and communicate risk analysis results effectively. An area closely related to uncertainties is sensitivity analysis. Sensitivity analysis involves the determination of the size and significance of the magnitude of changes in the risk estimates with respect to changes in individual input parameters. It is used to identify those data which need to be accurate, and those which are less sensitive and hence have less effect upon overall accuracy. Sources of uncertainty have to be identified whilst parameters to which the analysis is sensitive and the degree of sensitivity must be stated.

Table 2 A subset of the model output that shows that it identified and appropriately characterised the June and July 2007 heat wave events as extreme in the 1991–2009 NOA station database

Start date	T_{appmax}-T_{appmax}.p95	T_{max}	Duration (days)	Hazard score (out of 5.0)	Heat wave classification
20 June 2007	11.19	43.8	10	4.7	Extreme
19 July 2007	7.61	41.2	9	4.7	Extreme

Four parameters were altered (increased and decreased) to investigate the sensitivity of the hazard model: (1) the empirical temperature threshold of 37 °C for Athens, for identifying 'hot days'(Identification and extraction of hot days), (2) the 'psychological' air temperature threshold of 40 °C, which determines the heat wave intensity, (3) the air temperature field from the urban climate model (Urban Climate Model) which carries an uncertainty of approximately 1±2 °C (Manunta et al. 2011), and (4) the relative humidity field with an estimated 10 % uncertainty. The experiments were carried out for the warmest month in the dataset, namely June 2007. During the sensitivity analysis, one factor at a time was changed to see what effect this produces on the output heat wave hazard map. We started from the nominal values for the four parameters; then one input parameter was adjusted keeping others at their nominal value; subsequently, the value is returned, and the second parameter is deviated.

The sensitivity analysis results are shown in Fig. 10. The central map is the one with nominal values of (1) / (2) / (3) / (4), i.e. 37/40/AT/RH. It is noted that AT and RH are the fields for the whole study area. Red font denotes the deviation from the nominal values of the central panel. To assist readers, blue arrows mark the adjustment in the temperature threshold used in the definition of hot days (±1 °C), the red ones the adjustment in the 'psychological' threshold (±1 °C), the green ones the uncertainty in AT field (1±2 °C) and finally the purple arrows show the deviation in RH field (±10 %). The analysis revealed the following interesting findings:

- The empirical temperature threshold for the identification of hot days is critical to define the patterns of the areas affected by a heat wave within the greater study area. Lowering the threshold results in larger areas being affected (upper left panel of Fig. 10). In the centre, the hazard level is unchanged (average hazard is increased by 0.2 out of 5, i.e. 4.6 %) while in the whole image the average hazard is increased by 0.4, i.e. 8 %, therefore one has to be careful as to which threshold is to be used for a specific city as a low value will result in false alarms. Increasing the threshold has less effect on the patterns (lower right panel) and average city centre and whole area values; however, it lowers the hazard of high altitude areas.
- The 'psychological' air temperature threshold of 40 °C, which determines the heat wave intensity, is a parameter entering the fuzzy model to determine the intensity of an event. It affects less the distribution of heat wave hazard compared with the empirical temperature threshold, making the fuzzy model robust in the characterisation of severity of heat waves. Increasing the threshold from 40 to 41 °C (upper right panel) gives larger areas a lower severity, yet in relative change numbers this is negligible (of the order of 3 %). The city centre is not much affected in 1-degree fluctuations of the threshold (less than 1 %).
- The air temperature field was not deviated symmetrically from its nominal value in order to take into account a systematic bias of 1 °C (Manunta et al. 2011) against in situ measurements. The resultant maps (vertical middle panels) on heat wave severity are indeed very sensitive to the air temperature field, as expected. In particular, increasing the AT by 1 °C results in a 4.6 % increase in hazard, whilst decreasing it by 3 °C decreases the hazard by 30 %. This was by far the feature to which the model is most sensitive.
- Finally, the RH field can alter the heat wave hazard patterns as it is related to the dew point temperature and the apparent temperature thus accounting for the physiological impact of heat on health (see Eq. 1). The patterns of high hazard are altered (horizontal middle panels): A decrease of 10 % in RH results in a decrease of hazard in the city centre (remaining high along the western coastline) and the increase of 10 % results in more areas being under high hazard. It is important to note that neither of these changes is more than 1.5 % when the whole area is considered.

Given the sensitivity of the approach to the air temperature, it is fair to state that having accurate

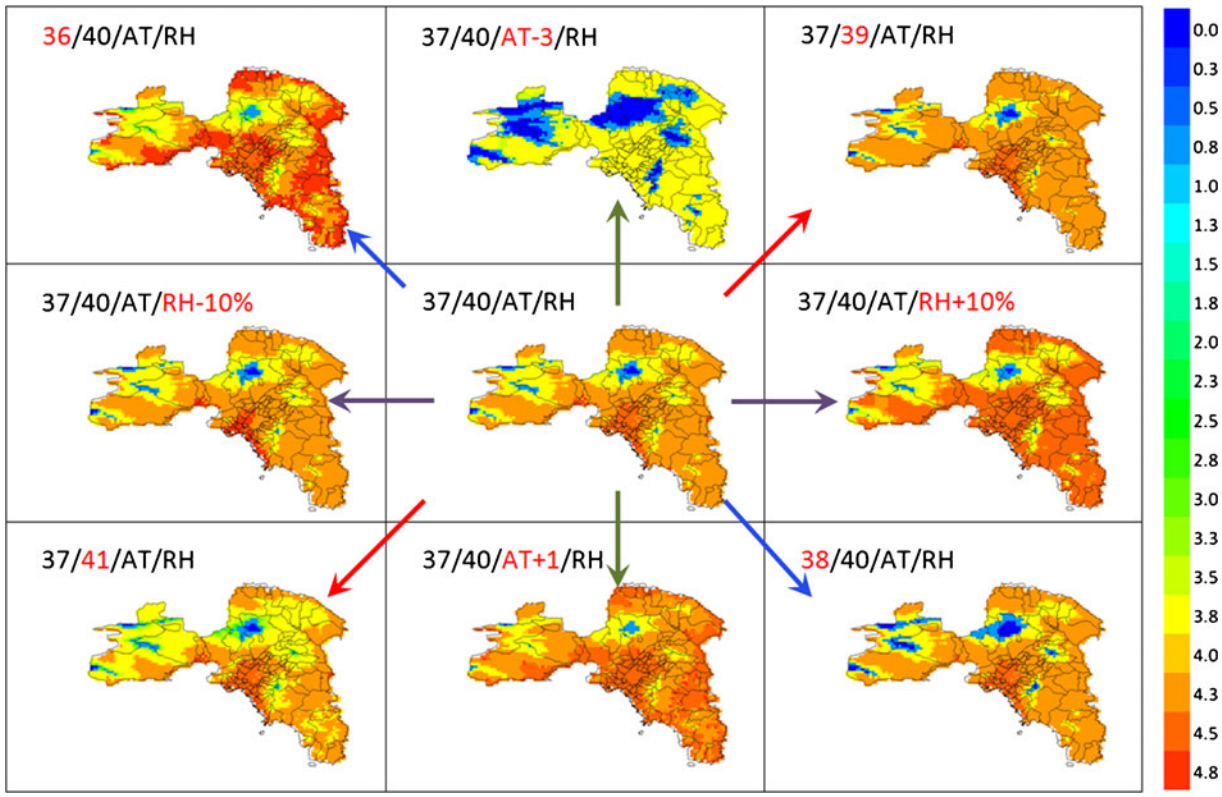

Fig. 10 Sensitivity analysis of the heat wave hazard model. The *central panel* represents the nominal values for June 2007. *Blue arrows* mark the adjustment in the temperature threshold used in the definition of hot days (±1 °C), the *red ones* the adjustment in the 'psychological' threshold (±1 °C), the *green ones* the uncertainty in AT field (1±2 °C) and finally the *purple arrows* show the deviation in RH field (±10 %). Modifications in the nominal values are shown with *red fonts*

and reliable air temperature estimates is very important. In Validity of model's individual components, we already discussed in more details the validation of the urban climate model. However, it is quite important to be aware of the difficulties in validation of urban air temperatures (Oke 2006) due to microscale effects, especially when comparing in situ measurements against $1 \times 1\text{-km}^2$ grid values.

Conclusions

Studies of past events in terms of distribution and assessment of risk are important tools to support decision makers, stakeholders and interested parties to agree on the preventative measures to take and to prepare in ways to avoid the immediate heat wave consequences, most notably in citizens' health as well as energy consumption of buildings for air-conditioning purposes. This article introduced a novel approach for mapping at intra-urban scale the heat wave hazard and risk based on a fuzzy logic concept. The methodology utilised a combination of state-of-the-art technologies, such as satellite remote sensing, urban climate modeling, artificial intelligence and advanced computing to produce monthly hazard and risk maps of past years. These maps show the hazard severity and the spatial distribution of risk within a city agglomeration and prove that there is a strong potential in the analysis for risk zoning.

The importance of the findings of this article is twofold: First, they give spatially distributed information on the heat wave severity and risk experienced in specific areas in Athens, Greece, during two severe events. This can be useful for targeted prevention measures (short-term planning) or even UHI mitigation planning at city level (long-term planning). In addition, the results are useful to energy providers. Secondly, the approach shown here offers a repeatable methodology that can be customised for other cities. The methodology does not need expensive or proprietary data to be applied.

Following Meehl and Tibaldi (2004) results, priority should be given to application to areas already experiencing strong heat waves (e.g. southwest, midwest and southeast United States and the Mediterranean region) but also to other areas (e.g. northwest United States, France, Germany and the Balkans) where increases of heat wave intensity could have more serious impacts because these areas are not currently as well adapted to heat waves.

As extreme heat events continue to cause preventable human mortality, approaches such as the classification scheme proposed in this study will be adopted as a foundation to understanding heat wave hazard and risk spatially for the purposes of saving lives and reducing economic losses. In collaboration with Civil Protection authorities, city planners and/or energy providers a major future task lies in the application to other cities and the downscaling to census block level. The latter holds especially for the air temperature modeling approach in which currently no microclimatic effects are taken into account. The combination, however, with producing long historic time series of urban air temperature fields makes this task rather challenging from a computational point of view.

Acknowledgements The authors thank Dr. Dimitra Founda from the Institute of Environmental Research and Sustainable Development of NOA for providing the station dataset and Ms. Maria Mihelaraki from the Hellenic National Meteorological Service for her contribution regarding heat waves in Athens. Census block data were provided by the Hellenic Statistical Authority (www.statistics.gr). The work was funded by the European Space Agency project 'Urban Heat Islands and Urban Thermography' (www.urbanheatisland.info; Grant no. 21913/08/I-LG). The authors wish to acknowledge the input from the anonymous reviewers, which substantially improved the manuscript.

References

Armstrong, B. G., Chalabi, Z., Fenn, B., Hajat, S., Kovats, S., Milojevic, A., et al. (2011). Association of mortality with high temperatures in a temperate climate: England and Wales. *Journal of Epidemiology and Community Health, 65*, 340–345.

Basu, R. (2009). High ambient temperature and mortality: A review of epidemiologic studies from 2001 to 2008, Review. *Environmental Health, 8*, 40.

Ca, V. T., Ashie, Y., & Asaeda, T. (2002). A k-ε turbulence closure model for the atmospheric boundary layer including urban canopy. *Boundary-Layer Meteorol, 102*, 459–490.

Choi, J., Chung, U., & Yun, J. I. (2003). Urban-effect correction to improve accuracy of spatially interpolated temperature estimates in Korea. *Journal of Applied Meteorology, 42*, 1711–1719.

Council of the European Union (2009). Council Conclusions on a community framework on disaster prevention within the EU, 2979th JUSTICE and HOME AFFAIRS Council meeting. Brussels, 30 November 2009.

Daglis, I.A., S. Rapsomanikis, K. Kourtidis, D. Melas, A. Papayannis, I. Keramitsoglou, T. Giannaros, V. Amiridis, G. Petropoulos, A. Georgoulias, J.-A. Sobrino, P. Manunta, J. Gröbner, M. Paganini, and R. Bianchi, "Results of the DUE Thermopolis campaign with regard to the Urban Heat Island (UHI) effect in Athens," in *Proc. ESA Living Planet Symposium*, ESA **SP-686**, European Space Agency (2010).

de Bruin, H. A. R., & Holtslag, A. A. M. (1982). A simple parameterization of surface fluxes of sensible and latent heat during daytime compared with the Penman–Monteith concept. *Journal Applications Meteorological, 21*, 1610–1621.

De Ridder, K. (2006). Testing Brutsaert's temperature roughness parameterization for representing urban surfaces in atmospheric models. *Geology-Physics Research Letters, 30*, L13403. doi:10.1029/2006GL026572.

De Ridder, K., & Schayes, G. (1997). The IAGL land surface model. *Journal of Applied Meteorology, 36*, 167–182.

Dee, D. P., et al. (2011). The ERA-Interim reanalysis: Configuration and performance of the data assimilation system. *Quarterly Journal of the Royal Meteorological Society, 137*, 553–597.

D'Ippoliti, D., et al. (2010). The impact of heat waves on mortality in 9 European cities: Results from the EuroHEAT project. *Environmental Health: A Global Access Science Source, 9*, 37.

Doucet, A., Freitas, N. D., & Gordon N. (2001). *Sequential Monte Carlo methods in practice*. Birkhauser, 2001.

Dousset, B., Gourmelon, F., Laaidi, K., Zeghnoun, A., Giraudet, E., Bretin, P., et al. (2011). Satellite monitoring of summer heat waves in the Paris metropolitan area. *International Journal of Climatology, 31*, 313–323. doi:10.1002/joc.2222.

Driankov, D., Hellendoorn, H., & Reinfrank, M. (1993). *An introduction to fuzzy control*. Berlin: Springer-Verlag.

Dupont, S., & Mestayer, P. (2006). Parameterization of the urban energy budget with the submesoscale soil model. *Journal of Applied Meteorology and Climatology, 45*, 1744–1765.

Easterling, D. R., Meehl, G. A., Parmesan, C., Changnon, S. A., Karl, T. R., & Mearns, L. O. (2000). Climate extremes: Observations, modeling and impacts (review). *Science, 289*, 2068–2074.

EC European Commission. (2010). *Commission staff working paper: Risk assessment and mapping guidelines for disaster management*. Brussels: SEC(2010) 1626 final.

EEA European Environment Agency. (2010). *Mapping the impacts of natural hazards and technological accidents in Europe: An overview of the last decade. Technical report No 13/2010* (pp. 1725–2237). Copenhagen: ISSN.

Founda, D., & Giannakopoulos, C. (2009). The exceptionally hot summer of 2007 in Athens, Greece—A typical summer in the future climate? *Global and Planetary Change, 67*, 227–236.

Gallo, K., & Owen, T. (1999). Satellite-based adjustments for the Urban Heat Island temperature bias. *Journal of Applied Meteorology, 38*, 806–813.

Garratt J.R. (1992). *The atmospheric boundary layer*, Cambridge University Press, Cambridge (1992).

Grimmond, C. S. B., & Oke, T. R. (2002). Turbulent heat fluxes in urban areas: Observations and a local-scale Urban

Meteorological Parameterization Scheme (LUMPS). *Journal Applied Meteorology, 41*, 792–810.

Harlan, S. L., Brazel, A. J., Prashad, L., Stefanov, W. L., & Larson, L. (2006). Neighborhood microclimates and vulnerability to heat stress. *Social Science & Medicine, 63*, 2847–2863.

Henschel, A., Burton, L. L., Margolis, L., & Smith, J. E. (1969). An analysis of the heat deaths in St. Louis during July, 1966. *American Journal of Public Health, 59*, 2232–2242.

IPCC Intergovernmental Panel on Climate Change (2007). Contribution of Working Groups I, II and III to the Fourth Assessment Report of the Intergovernmental Panel on Climate Change, Core Writing Team, Pachauri, R.K. and Reisinger, A. (Eds.), IPCC, Geneva, Switzerland. pp 104 (http://www.ipcc.ch/publications_and_data/ar4/syr/en/contents.html).

ISO International Organization for Standardization 31010:2009 Risk management—Principles and guidelines http://www.iso.org/iso/catalogue_detail?csnumber=43170.

Jarvis, C. H., & Stuart, N. (2001a). A comparison among strategies for interpolating maximum and minimum daily air temperatures. Part I: The selection of "guiding" topographic and land cover variables. *Journal of Applied Meteorology, 40*, 1060–1074.

Jarvis, C. H., & Stuart, N. (2001b). A comparison among strategies for interpolating maximum and minimum daily air temperatures. Part II: The interaction between number of guiding variables and the type of interpolation method. *Journal of Applied Meteorology, 40*, 1075–1084.

Johnson, D. P., & Wilson, J. S. (2009). The socio-spatial dynamics of extreme urban heat events: The case of heat-related deaths in Philadelphia. *Applied Geography, 29*, 419–434. doi:10.1016/j.apgeog.2008.11.004.

Katsouyanni, K., Trichopoulos, D., Zavitsanos, X., & Touloumi, G. (1988). The 1987 Athens heatwave. *Lancet, 2*, 573.

Keramitsoglou, I., Daglis, I. A., Amiridis, V., Chrysoulakis, N., Ceriola, G., Manunta, P., et al. (2012). Evaluation of satellite-derived products for the characterization of the urban thermal environment. *Journal of Applied Remote SensingSpecial Issue: Advances in Remote Sensing for Monitoring Global Environmental Changes, 6*, 061704.

Keramitsoglou, I., Kiranoudis, C. T., Ceriola, G., Weng, Q., & Rajasekard, U. (2011). Identification and analysis of urban surface temperature patterns in Greater Athens, Greece, using MODIS imagery. *Remote Sensing of Environment, 115*(3080–3090), 2011.

Kusaka, H., Kondo, H., Kikegawa, Y., & Kimura, F. (2001). A simple single-layer urban canopy model for atmospheric models: Comparison with multi-layer and SLAB models. *Boundary-Layer Meteorol., 101*, 329–358.

Laaidi, K., et al. (2011). The impact of heat islands on mortality in Paris during the August 2003 heatwave. *Environ Health Perspect, 120*, 2. doi:10.1289/ehp.1103532.

LSA SAF (2010), Down-welling longwave flux (DSLF) product user manual, Issue 3.3, Sept. 2010 (Available on http://landsaf.meteo.pt).

LSA SAF (2011), Down-welling surface shortwave flux (DSSF) product user manual, Issue 2.6v2, July 2011 (Available on http://landsaf.meteo.pt).

Maiheu, B., Ridder, K. D., Dousset, B., Manuta, P., Ceriola, G., Viel, M., Daglis, I. A., et al. (2010). Modelling air temperature via assimilation of satellite derived surface temperature within the Urban Heat Island Project. In *EARSel Workshop Proceedings of the Joint SIG Workshop Urban–3D–Radar–Thermal Remote Sensing and Developing Countries*, 162–181.

Mamdani, E. H. (1974). Application of fuzzy algorithms for simple dynamic plants. *Proceedings of IEE, 121*(12), 1585–1588.

Manunta et al. (2010a). Design justification file v.4, ESA project: "Urban Heat Island and thermography"—Contract number 21913/08/I-LG.

Manunta, P., Ceriola, G., Daglis, I. A., de Ridder, K., Giannaros, T., Keramitsoglou et al. (2010b). Urban Heat Islands and urban thermography. In *Proc. ESA Living Planet Symposium*, ESA SP-686, European Space Agency.

Manunta et al. (2011). Product validation report v.3, ESA Project: "Urban Heat Island and thermography"—Contract number 21913/08/I-LG.

Martilli, A., Clappier, A., & Rotach, M. W. (2002). An urban surface exchange parameterisation for mesoscale models. *Boundary-Layer Meteorol., 104*, 261–304.

Masson, V. (2000). A physically-based scheme for the urban energy budget in atmospheric models'. *Boundary-Layer Meteorol., 98*, 357–397.

McMichael, A. J., Wilkinson, P., Kovats, R. S., Pattenden, S., Hajat, S., Armstrong, B., et al. (2008). International study of temperature, heat and urban mortality: The 'ISOTHURM' project. *International Journal of Epidemiology, 37*, 1121–1131.

Meehl, G. A., & Tibaldi, C. (2004). More intense, more frequent, and longer lasting heat waves in the 21st century. *Science, 305*, 994–997.

Metaxas, D. A., & Kallos, G. (1980). Heat waves from a synoptic point of view. *Rivista di Meteorologia Aeronautica JL, 2–3*, 107–119.

Oke, T. R., Johnson, D. G., Steyn, D. G., & Watson, I. D. (1991). Simulation of surface urban heat island under ideal conditions at night—Part 2: Diagnosis and causation. *Boundary Layer Meteorology, 56*, 339–358.

Oke, T. R. (2006). Initial guidance to obtain representative meteorological observations at urban sites. WMO Instruments and Observing Methods, Report No 81, WMO/TD-No. 1250 (Available at http://www.wmo.int/pages/prog/www/IMOP/publications/IOM-81/IOM-81-UrbanMetObs.pdf).

Patz, J. A., Campbell-Lendrum, D., Holloway, T., & Foley, J. A. (2005). Impact of regional climate change on human health. *Nature, 438*, 310–317.

Rigo, G., & Parlow, E. (2007). Modelling the ground heat flux of an urban area using remote sensing data. *Theoretical and Applied Climatology, 90*, 185–199.

Roberts, S., Oke, T. R., Grimmond, C. S. B., & Voogt, J. (2006). Tests of four methods to estimate urban heat storage in central Marseille. *Journal of Applied Meteorology and Climatology, 45*, 1766–1781.

Ruddell, D.M., Harlan, S.L., Grossman-Clarke, S., & Buyantuyev, A. (2010). Risk and exposure to extreme heat in microclimates of Phoenix, AZ. In *Geospatial techniques in urban hazard and disaster analysis*, P.S. Showalter, Y. Lu (eds.), Geotechnologies and the environment 2, doi 10.1007/978-90-481-2238-7_9, Springer Science+ Business Media B.V. 2010.

Schuman, S. H. (1972). Patterns of urban heat-wave deaths and implications for prevention: Data from New York and St. Louis during July 1996. *Environmental Researc, h, 5*, 59–75.

Semenza, J. C., McCullough, J. E., Flanders, W. D., McGeehin, M. A., & Lumpkin, J. R. (1999). Excess hospital admissions during the July 1995 heat wave in Chicago. *American Journal of Preventive Medicine, 16*(4), 269–277.

Shamrock, W. C., Klemp, J. B., Dudhia, J., Gill, D. O., Barker, D. M., Wang, W., Powers, J. G., et al. (2005). A description of the advanced research WRF Version 2. NCAR Technical Note.

Smoyer, K. (1998). Putting risk in its place: Methodological considerations for investigating extreme event health risk. *Social Science & Medicine, 47*, 1809–1824.

Theoharatos, G., Pantavou, K., Mavrakis, A., Spanou, A., Katavoutas, G., Efstathiou, P., et al. (2010). Heat waves observed in 2007 in Athens, Greece: Synoptic conditions, bioclimatological assessment, air quality levels and health effects. *Environmental Research, 110*(2), 152–161.

WMO World Meteorological Organization (2008). Heat–health action plans, edited by Franziska Matthies, Graham Bickler, Neus Cardeñosa Marín and Simon Hales. ISBN 978 92 890 7191 8 http://www.euro.who.int/en/what-we-publish/abstracts/heathealth-action-plans.

WMO World Meteorological Organization (2011). Weather extremes in a changing climate: Hindsight on foresight, ISBN: 978-92-63-11075-6, http://www.wmo.int/pages/mediacentre/news/documents/1075_en.pdf.

Zadeh, L. A. (1965). Fuzzy sets. *Information and control, 8*, 338–353.